

# BEAM HALO FORMATION WITH DIFFERENT CATHODE DISTRIBUTIONS\*

I. Neththikumara<sup>†</sup>, K. Deitrick, B. R. Gamage, R. Rimmer, T. Satogata, N. Sereno, S. Setiniyaz

Thomas Jefferson National Accelerator Facility, Newport News, VA, USA

W. Bergan, E. Wang, Brookhaven National Lab, Upton, NY, USA

N. Wang, Cornell University, Ithaca, NY, USA

## Abstract

Beam halo is the low-density distribution of particles extending beyond the beam core, and its generation and mitigation are important topics in particle accelerator design. In particular, effective mitigation of beam halo is essential for the hadron cooler design based on Energy Recovery Linac (ERL), which is being developed to suppress emittance growth in high energy proton beams in the Electron-Ion Collider. The ERL is required to deliver an electron beam with average beam current of 100 mA and a bunch charge of 1 nC. In the ERL injector and booster-linac, space charge effects are stronger due to the relatively low beam energy (6 MeV). Additionally, the longer bunch length of approximately 100 ps in this regime *vs* the RF period of 5.08 ns makes the formation of beam halos more likely. Therefore, effective collimation of beam halo is critical for maintaining the required beam parameters. To design an effective collimation scheme, several halo distributions were generated at the cathode and used to study halo formation within the injector-merger. This paper presents different halo distributions and halo formation, providing insights on halo collimation strategy.

## INTRODUCTION

A Strong Hadron Cooler (SHC) based on an Energy Recovery Linac (ERL) is a possible solution to cool high energy proton beams in the U.S. Electron-Ion Collider (EIC), with the goal of mitigating emittance growth and meeting high-luminosity requirements of the EIC. This ERL cooler is designed to operate in two distinct modes (modes A & B), to cool down hadron beams with energies 100 GeV and 275 GeV. Electron beam of an average current 100 mA is used with peak bunch currents of 10 A and 13 A for mode A and mode B, respectively. Electron beam energies at the entrance to the cooling section are 55 MeV and 150 MeV so that the velocities of both hadrons and co-propagating electrons are equal. A schematic of the SHC-ERL is given in Fig. 1 [1, 2].

Cooling effectiveness depends on maintaining the quality of the intense, high current electron beam as it transported through the SHC-ERL towards the cooling sections. Higher current beams tend to create beam halo due to intense space charge fields, magnet misalignment and imperfections, orbit

misalignment and steering errors and RF errors. Beam halo is usually defined as the low-density particle distribution formed around the denser beam core. These halos create problems in maintaining quality beam transport and could cause radiation damage to beamline equipment. Mitigation of halo formation and propagation is critical for machine protection, while maintaining proper beam transport.

## HALO FORMATION AT CATHODE

Halo formation at the cathode occurs due to multiple reasons, creating halo in both transverse and longitudinal phase space.

- Larger cathode response time resulting longer tails, eventually contributes to formation of beam halo [3].
- Degradation of cathode material leads surface imperfections, affecting its quantum efficiency (QE). This could lead to increased thermal emittance or non-uniform electron emission that could eventually create beam halo.
- Mismatch of the cathode spot size influences create beam halo as this strongly affects important beam properties such as beam brightness, emittance, energy spread and space charge effects [4].

If the density functions of the core and halo are given by  $\rho_1$  and  $\rho_2$ , then the beam density with halo is expressed as

$$\rho(r) = \rho_1 \exp\left(\frac{r}{\sigma_1 \sqrt{2}}\right)^2 + \rho_2 \exp\left(\frac{r}{\sigma_2 \sqrt{2}}\right)^2, \quad (1)$$

where  $\rho_2 \leq \rho_1$  and  $\sigma_2 \geq \sigma_1$  [9]. Here  $\rho_{(1,2)}$  define the amplitudes of the two density profiles, while  $r$  denotes the radius.

Beam halo studies in the SHC-ERL is limited to the beam dynamics during its design phase. We used Distgen package [5] to generate the distributions and Bmad [6] for tracking studies and implementing collimation scheme.

## Core Beam

The core beam used in SHC-ERL tracking studies has a radially truncated, beer-can-shaped distribution with a total charge of 1 nC, as illustrated in Fig. 2. The mean transverse energy is 130 meV. The beam accelerates to approximately 400 keV at the injector gun, with an average beam current of 100 mA. The transverse distribution is Gaussian with a

\* This work is supported by Jefferson Science Associates, LLC under U.S. DOE Contract DE-AC05-06OR23177 and Brookhaven Science Associates, LLC, Contract DESC0012704

<sup>†</sup> isurunh@jlab.org

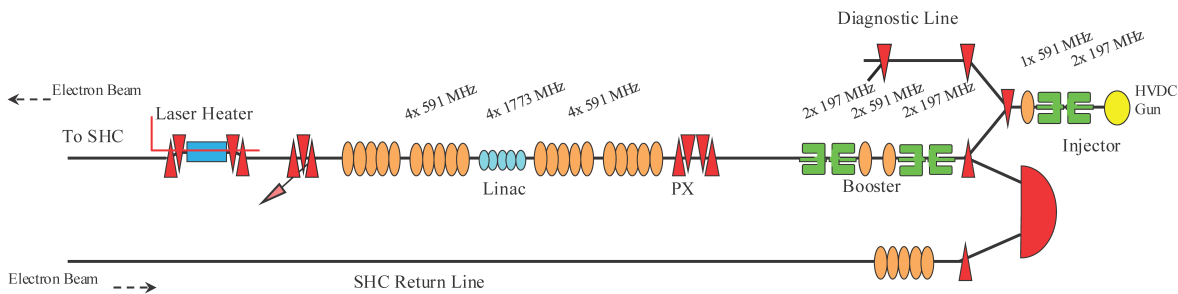


Figure 1: Conceptual design layout of the SHC-ERL with the main components of the ERL lattice; injector, booster, main linac and return line.

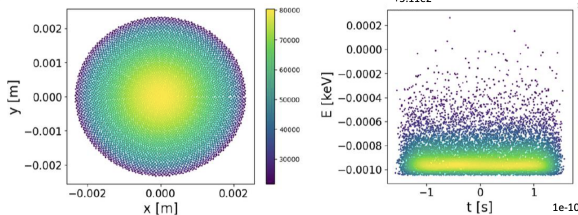


Figure 2: Transverse and longitudinal space of the core beam distribution at the cathode. Total energies of the particles is given in the energy axis.

truncation radius of 2.3 mm, longitudinal distribution is a 10<sup>th</sup> order super-Gaussian, with a  $\sigma_t = 82.87$  ps [7].

### Halo Beam

The halo distribution consists of both transverse and longitudinal particles and is created by superimposing multiple distributions. The core beam remained unchanged, while the parameters for the halo particles are varied to generate multiple distinct distributions. According to the literature, the halo current is typically in between 0.1–1.0% of the core beam [3]. We used a halo distribution with charge of 1 pC. Transverse halo can exhibit various distribution types. Particles extending beyond the core beam's truncation radius may follow uniform, radial-Gaussian, or hollow distributions [8].

The initial distribution with transverse and longitudinal halo used for tracking is shown in Fig. 3. The initial halo distribution was defined with  $N = 200,000$  particles and a charge of  $Q = 1$  pC, the truncated halo-tail retains only  $N = 48,929$  particles and a reduced charge of  $Q = 0.2446$  pC. This specific distribution is chosen to minimize temporal overlap between the core and halo, resulting in a distinct, tail-like halo structure.

A denser tail is observed in Fig. 3 (right). However, it is important to note that the macro-particle charge in the halo region is 0.1% lower than that of the core beam, resulting in a significantly reduced halo current. For simulation purposes, a larger number of halo particles is preferred to improve statistical resolution; therefore, the macro-particle

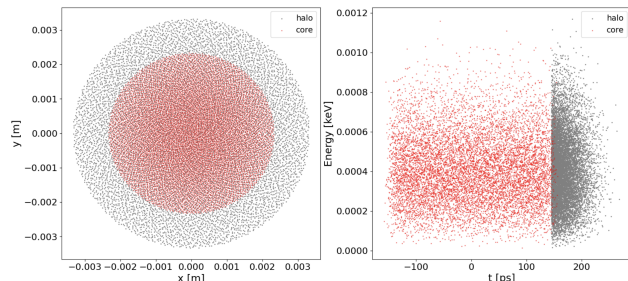


Figure 3: Transverse and longitudinal space of the combined beam.

charges differ between the core and halo distributions. The above distribution is tracked from cathode to the end of the injector-merger through the lattice optimized for smooth beam transportation of the space charge dominated beam.

### Halo Tracking With Space Charge Effects

With no collimators placed in the beam line, halo formation using a truncated radially-Gaussian cathode distribution is observed. Figure 4 illustrates the beam phase space at the end of injector-merger, where the core and halo particles are marked with two different colors.

As illustrated, the halo particles disperse more in both transverse and longitudinal directions. However, in longitudinal phase space, the tail exhibits a curvature distinct from the core beam. Several studies were performed to explain this longitudinal behavior. Effective space charge fields are stronger in regions where the core and halo overlap, due to the higher charge density. In contrast, these fields weaken in low-charge-density regions, such as the halo tail. The core is more uniform than the halo, and particles near the beam core experience a uniform RF curvature within the RF cavities, resulting in a smaller curvature than the halo tail.

Particle beam with halo is tracked through the injector line both with and without space charge effects. The magnet and RF parameters in the injector-merger line is optimized to transport the design space charge dominated core beam describe in [10]. However, even with purely transverse halo at cathode, a significant difference is observed between

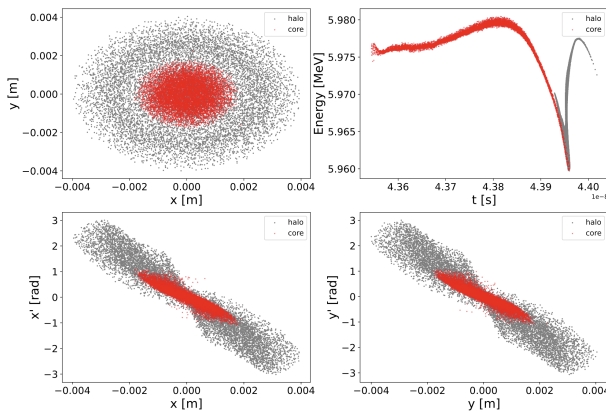


Figure 4: Halo formation with space charge fields enabled, at the end of the merger line, using the initial distribution shown in Fig. 3.

tracking with and without space charge. Figure 5 illustrates comparison beam phase spaces at the end of the injector cryomodule.

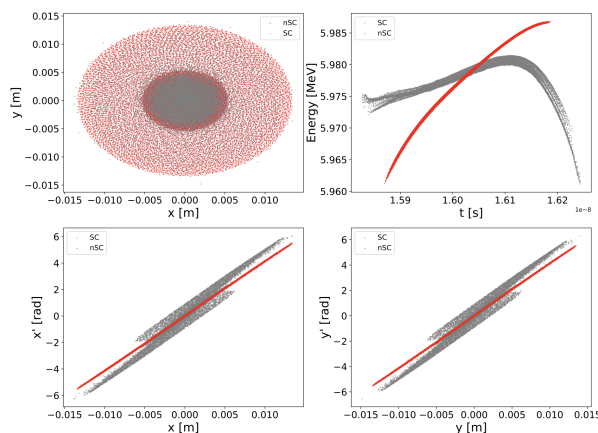


Figure 5: Comparison of the beam phase space with (gray) and without (red) space charge fields.

The design energy at this location is 6 MeV. Compared to the transverse profiles, the longitudinal profiles show a more pronounced difference between tracking with and without space charge. Both the bunch length and energy spread are smaller in the absence of space charge fields effects. It is important to note that the magnet and rf parameters are set to minimize the energy spread of the core beam with effects of space charge fields. Under strong space charge forces, particles experience strong transverse repulsion, as the transverse space charge force exceeds the longitudinal component. This typically result in a pencil-shaped beam with a high aspect ratio. This behavior is clearly observed in Fig. 6. Phase advance of the beam is calculated using

$$\Phi(z) = \int_{z1}^{z2} \frac{dz}{\omega^2(z)}, \quad (2)$$

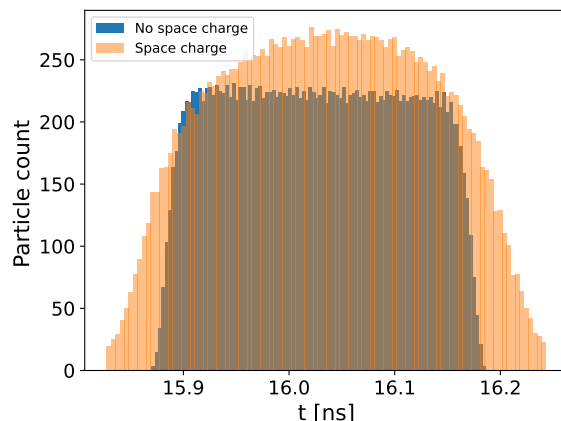


Figure 6: Comparison of the particle density profiles tracked with and without space charge fields.

where  $\omega(z)$  is the amplitude function given by

$$\omega'' + \kappa \omega - \frac{1}{\omega^3} = 0. \quad (3)$$

The phase advance of particles decreases under the influence of space charge fields, as these fields act as a defocusing force on the beam [11]. When the beam is tracked without accounting for its self-fields, it experiences artificially stronger focusing forces, leading to mismatched phase-space ellipses in both the horizontal and vertical planes, as observed in Fig. 5.

## CONCLUSION

Formation of halo distribution at cathode in both longitudinal and transverse dimensions is considered when creating the halo beam distribution at the cathode. Low-density and low-current halo particles are integrated into the main core beam and observed its propagation through the injection merger, in the space charge optimized lattice. Incorporating space charge effects in tracking studies confirms that the lattice is effectively designed for smooth propagation and control of the design core beam. Space charge effects are smaller for the halo distribution due to its low current density. Hence, a tail is formed with a larger curvature than the core beam. The difference in phase advance experienced by particles with and without space charge fields leads to significant variations in phase space, resulting in distinct halo profiles. Uncontrolled halo particles could lead to beam blow-up, particle losses and potential damage the beamline components. As a next step in this work, we have initiated a study focused on developing an effective halo collimation scheme.

## REFERENCES

- [1] C. Gulliford *et al.*, “Design and optimization of an ERL for cooling EIC hadron beams”, in *Proc. 14th Int. Particle Accelerator Conf. (IPAC’23)*, Venice, Italy, May 2023, pp. 73–76. doi:10.18429/JACoW-IPAC2023-MOPA016

- [2] K. Deitrick *et al.*, “Development of an ERL for coherent electron cooling at the Electron-Ion Collider”, in *Proc. IPAC’24*, Nashville, TN, USA, May 2024, pp. 3086–3089.  
doi:10.18429/JACoW-IPAC2024-THPC40
- [3] O. Tanaka *et al.*, “New halo formation mechanism at the KEK compact energy recovery linac”, *Phys. Rev. Spec. Top. Accel. Beams*, vol. 21, p. 024202, 2018.  
doi:10.1103/PhysRevAccelBeams.21.024202
- [4] P. Piot and D. Mihalcea, “Analysis of halo formation in a DC photoinjector”, in *Proc. LINAC’08*, Victoria, Canada, Sep.-Oct. 2008, paper TUP103, pp. 645–647.
- [5] C. Gulliford, “Distgen — particle distribution generator”, github: <https://colwyngulliford.github.io/distgen/>
- [6] D. Sagan, “Bmad: A relativistic charged particle simulation library”, *Nucl. Instrum. Meth.*, vol. A558, pp. 356–359, 2006.  
doi:10.1016/j.nima.2005.11.001
- [7] N. Wang *et al.*, “Optimization of cooling distribution of the EIC SHC cooler ERL”, in *Proc. IPAC’24*, Nashville, USA, May 2024, pp. 1101–1104.  
doi:10.18429/JACoW-IPAC2024-TUPC43
- [8] I. Neththikumara *et al.*, “Halo beam generation at the gun cathode for the SHC ERL”, JLAB Newport News, VA, USA, Rep. JLAB-TN-24-048, 2024.
- [9] P. A. P. Nghiêm, N. Chauvin, N. Pichoff, D. Uriot, and M. Valette, “Core-halo limit as an indicator of high-intensity beam internal dynamics”, in *Proc. IPAC’15*, Richmond, VA, USA, May 2015, pp. 86–88.  
doi:10.18429/JACoW-IPAC2015-MOPWA006
- [10] I. Neththikumara *et al.*, “Space-charge studies on strong hadron cooler energy recovery linac”, presented at NAPAC’25, Sacramento, CA, USA, paper TUP091, this conference.
- [11] M. Reiser, ”Theory and Design of Charged Particle Beams”, Wiley-VCH Verlag GmbH & Co., second edition.  
doi:10.1002/9783527622047